Large Deviations of Surface Height in the Kardar-Parisi-Zhang Equation

Baruch Meerson,* Eytan Katzav,† and Arkady Vilenkin‡
Racah Institute of Physics, Hebrew University of Jerusalem, Jerusalem 91904, Israel
(Received 15 December 2015; published 19 February 2016)

Using the weak-noise theory, we evaluate the probability distribution $\mathcal{P}(H,t)$ of large deviations of height H of the evolving surface height $h(x,t)$ in the Kardar-Parisi-Zhang equation in one dimension when starting from a flat interface. We also determine the optimal history of the interface, conditioned on reaching the height H at time t. We argue that the tails of $\mathcal{P}$ behave, at arbitrary time $t>0$, and in a proper moving frame, as $-\ln\mathcal{P}\sim|H|^{5/2}$ and $\sim|H|^{3/2}$. The $3/2$ tail coincides with the asymptotic of the Gaussian orthogonal ensemble Tracy-Widom distribution, previously observed at long times.

DOI: 10.1103/PhysRevLett.116.070601

The Kardar-Parisi-Zhang (KPZ) equation [1] is the standard model of nonequilibrium interface growth driven by noise [2–6]. In $d=1$, the KPZ equation reads

$$\partial_t h=\nu\partial_x^2 h+(\lambda/2)(\partial_x h)^2+\sqrt{D}\xi(x,t), \tag{1}$$

where $h(x,t)$ is the interface height, and $\xi(x,t)$ is a Gaussian white noise with zero mean and $\langle\xi(x_1,t_1)\xi(x_2,t_2)\rangle=\delta(x_1-x_2)\delta(t_1-t_2)$. We will assume here that $\lambda<0$ [7].

At long times, the evolving KPZ interface exhibits self-affine properties and universal scaling exponents [2–4]. In $d=1$, its characteristic width grows as $t^{1/3}$, whereas the correlation length in the x direction grows as $t^{2/3}$, as confirmed in experiments [8]. The exponents $1/3$ and $2/3$ distinguish the KPZ universality class from the Edwards-Wilkinson (EW) universality class that corresponds to the absence of the nonlinear term in Eq. (1).

Recent years have witnessed spectacular progress in the exact analytical solution of Eq. (1); see Refs. [5] and [6] for reviews. For an initially flat interface, most often encountered in experiment, the exact height distribution at a given time was obtained by Calabrese and Le Doussal [9]. They achieved it by mapping Eq. (1) onto the problem of equilibrium fluctuations of a directed polymer with one end fixed, and the other end free, and by using the Bethe ansatz for the replicated attractive boson model [9]. They derived a generating function of the probability distribution $\mathcal{P}(H,t)$ of height H of the evolving KPZ interface in the form of a Fredholm Pfaffian. They also showed that, for typical fluctuations, and in the long-time limit, $\mathcal{P}(H,t)$ converges to the Gaussian orthogonal ensemble (GOE) Tracy-Widom (TW) distribution. Later on Gueudré *et al.* [10] used the exact results of Ref. [9] to extract the first four cumulants of $\mathcal{P}(H,t)$ in the *short-time* limit. These cumulants exhibit a crossover from the EW to the KPZ universality class as one moves away from the body of the distribution toward its (asymmetric) tails. The tails themselves, however, are unknown: neither for long, nor for short times. Finding them is a natural next step in the study of the KPZ equation, and it is our main objective here.

Instead of extracting the tails from the (quite complicated) exact solution [9], we will obtain them, up to pre-exponential factors, from the weak-noise theory (WNT) of Eq. (1). The WNT grew from the Martin-Siggia-Rose path-integral formalism in physics [11] and the Freidlin-Wentzel large-deviation theory in mathematics [12]. Being especially suitable for sufficiently steep distribution tails, it has been applied to turbulence [13], lattice gases [14], stochastic reactions [15] and other areas, including the KPZ equation itself [16]. To evaluate $\mathcal{P}(H,T)$, we first determine the optimal history of the interface conditioned on reaching the height H at time T. We find that the tails of $\mathcal{P}$ behave, at any time $T>0$ and in a proper moving frame [17], as $-\ln\mathcal{P}\sim H^{5/2}$ as $H\to\infty$ and $\sim|H|^{3/2}$ as $H\to-\infty$. The $3/2$ tail coincides with the asymptotic of the GOE TW distribution, previously established for long times [9]. We also reproduce the short-time asymptotics of the second and third cumulants of $\mathcal{P}(H,T)$, obtained in Ref. [10].

(i) *Scaling.*— Upon the rescaling transformation $t/T\to t$ $x/\sqrt{\nu T}\to x$, and $|\lambda|h/\nu\to h$ Eq. (1) becomes

$$\partial_t h=\partial_x^2 h-(1/2)(\partial_x h)^2+\sqrt{\epsilon}\xi(x,t), \tag{2}$$

where $\epsilon=D\lambda^2\sqrt{T}/\nu^{5/2}$ is a dimensionless parameter. Without loss of generality, we assume that the interface height H is reached at $x=0$. The initial condition is $h(x,t=0)=0$. Clearly, $\mathcal{P}(H,T)$ depends only on the two parameters $|\lambda|H/\nu$ and ϵ [17].

(ii) *Weak-noise theory.*— The WNT assumes that ϵ is small (more precise conditions are discussed below). Then a saddle-point evaluation of the proper path integral of Eq. (2) leads to a minimization problem for the action [16,19]. Its solution involves solving Hamilton equations for the optimal history of the height $h(x,t)$ and the canonically conjugate "momentum" field $\rho(x,t)$:

$$\partial_t h=\delta\mathcal{H}/\delta\rho=\partial_x^2 h-(1/2)(\partial_x h)^2+\rho, \tag{3}$$

$$\partial_t\rho=-\delta\mathcal{H}/\delta h=-\partial_x^2\rho-\partial_x(\rho\partial_x h), \tag{4}$$

where $\mathcal{H} = \int dx w$ is the Hamiltonian, and $w(x,t) = \rho[\partial_x^2 h - (1/2)(\partial_x h)^2 + \rho/2]$. The boundary conditions are $h(x,0) = 0$ and $h(x \to \pm\infty, t) = \rho(x \to \pm\infty, t) = 0$. The condition $h(0,1) = H$ translates into [19]:

$$\rho(x,1) = \Lambda\delta(x). \tag{5}$$

The *a priori* unknown coefficient Λ is ultimately determined by H.

Once the WNT problem is solved, one can evaluate

$$-\ln \mathcal{P}(H,T) \simeq \frac{S(\frac{|\lambda|H}{\nu})}{\epsilon} = \frac{\nu^{5/2}}{D\lambda^2\sqrt{T}} S\left(\frac{|\lambda|H}{\nu}\right), \tag{6}$$

where, in the rescaled variables, the action S is

$$S = \int_0^1 dt \int dx(\rho\partial_t h - w) = \frac{1}{2}\int_0^1 dt \int dx \rho^2(x,t). \tag{7}$$

Figure 1 shows $S = S(H)$ found by solving Eqs. (3) and (4) numerically with a modified version of the Chernykh-Stepanov iteration algorithm [20]. Analytic progress is possible in three limits that we now consider.

(iii) $H \to +\infty$, *or* $\Lambda \to +\infty$.— Here we drop the diffusion terms in Eqs. (3) and (4) and arrive at

$$\partial_t \rho + \partial_x(\rho V) = 0, \tag{8}$$

$$\partial_t V + V\partial_x V = \partial_x \rho. \tag{9}$$

where $V(x,t) = \partial_x h(x,t)$. Equations (8) and (9) describe a nonstationary inviscid flow of an effective gas with density ρ, velocity V, and *negative* pressure $p(\rho) = -\rho^2/2$ [21]. This hydrodynamic problem should be solved subject to the conditions $V(x,0) = 0$ and Eq. (5). An additional, "inviscid" rescaling $x/\Lambda^{1/3} \to x$, $V/\Lambda^{1/3} \to V$, and $\rho/\Lambda^{2/3} \to \rho$ leaves Eqs. (8) and (9) invariant, but makes the problem parameter-free, as Eq. (5) becomes $\rho(x,1) = \delta(x)$, describing the collapse of a gas cloud of unit mass into the origin at $t = 1$. Further, Eq. (7) yields

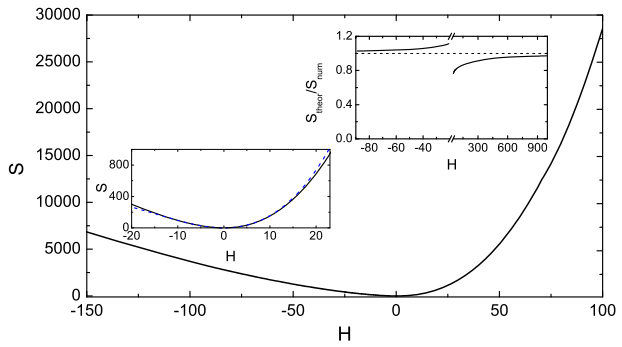

FIG. 1. The action S vs the rescaled height H; see Eq. (6). Main figure: numerics. Right inset: convergence of Eqs. (20) and (25) to numerical results at large $|H|$. Left inset: the small-H asymptotic (37) vs numerics.

$$S = \Lambda^{5/3} s, \tag{10}$$

where s should be obtained by plugging the solution $\rho(x,t)$ of the parameter-free problem into Eq. (7). Remarkably, we can already predict the scaling behavior of $S(H)$. Indeed, the rescaled height at $t = 1$ is $h(0,1) \equiv H_1 = |\lambda|H/(\nu\Lambda^{2/3})$. Therefore, $\Lambda = (|\lambda|/\nu)^{3/2}(H/H_1)^{3/2}$, and Eq. (10) yields

$$S(|\lambda|H/\nu) = (s/H_1^{5/2})(|\lambda|H/\nu)^{5/2}, \tag{11}$$

leading to the announced $H^{5/2}$ tail. What is left is to calculate s and H_1, which are both $\mathcal{O}(1)$. Fortunately, the hydrodynamic flow is quite simple:

$$V(x,t) = -a(t)x, \qquad |x| \le \ell(t), \tag{12}$$

and

$$\rho(x,t) = \begin{cases} r(t)\,[1 - x^2/\ell^2(t)], & |x| \le \ell(t), \quad (13) \\ 0, & |x| > \ell(t), \quad (14) \end{cases}$$

where $r(t) > 0$, $\ell(t) \ge 0$ and $a(t) \ge 0$ are functions of time to be determined. [The behavior of $V(x,t)$ at $|x| > \ell(t)$ will be discussed shortly.]

The "mass" conservation, inherent in Eq. (8), yields a simple relation $\ell(t)r(t) = 3/4$. Using it, and plugging Eqs. (12) and (13) into Eqs. (8) and (9), we obtain two coupled equations for $r(t)$ and $a(t)$: $\dot{r} = ra$ and $\dot{a} = a^2 + (32/9)r^3$. Their first integral is $a = (8/3)r\sqrt{r - r_0}$, where $r_0 \equiv r(0)$. This yields a single equation for $r(t)$: $\dot{r} = (8/3)r^2\sqrt{r - r_0}$. Its implicit solution, subject to $r(t \to 1) = \infty$, is

$$t = t(r) = \frac{3\sqrt{r - r_0}}{8rr_0} + \frac{2}{\pi}\arctan\left(\sqrt{\frac{r}{r_0} - 1}\right), \tag{15}$$

where $r_0 = (3\pi/16)^{2/3}$. Now we can calculate s:

$$s = \frac{1}{2}\int_0^1 dt \int_{-\ell}^{\ell} dx r^2(t)[1 - x^2/\ell(t)^2]^2 = \frac{2}{5}\int_0^1 dt r(t) = \frac{2}{5}\int_0^\infty dr r \frac{dt}{dr} = \frac{1}{5}\left(\frac{3\pi}{2}\right)^{2/3}. \tag{16}$$

What happens at $|x| > \ell(t)$, where $\rho = 0$? In the *static* regions, $|x| > \ell_0 \equiv 3/(4r_0) = 3^{1/3}(2/\pi)^{2/3}$, one has $\rho(x,t) = V(x,t) = h(x,t) = 0$ at all times. In the Hopf regions, $\ell(t) < |x| < \ell_0$, $V(x,t)$ is described by the (deterministic) Hopf equation $\partial_t V + V\partial_x V = 0$. Its solution is $x - Vt = F(V)$ [22], where the function $F(V)$ is found from matching with the pressure-driven solution at $x = \pm\ell(t)$:

$$F(V) = -\ell_0\left(1 + \frac{\sqrt{\ell_0}V}{\sqrt{3}}\arctan\frac{\sqrt{\ell_0}V}{\sqrt{3}}\right)\mathrm{sgn}V. \tag{17}$$

At $t = 1$ the pressure-driven flow shrinks to the origin, and the Hopf solution,

$$x(V) = V - \ell_0\left(1 + \frac{\sqrt{\ell_0}V}{\sqrt{3}}\arctan\frac{\sqrt{\ell_0}V}{\sqrt{3}}\right)\mathrm{sgn}V, \quad (18)$$

holds in the whole interval $|x| \le \ell_0$. Now we can find the optimal height profile $h(x, t = 1)$. For $-\ell_0 \le x \le 0$

$$h(x,1) = \int_{-\ell_0}^{x} V(x,1)dx = \int_0^V dV(dx/dV)V$$
$$= \frac{\sqrt{\ell_0}(3 - \ell_0 V^2)\arctan(\frac{\sqrt{\ell_0}V}{\sqrt{3}}) + \sqrt{3}V(V - \ell_0)}{2\sqrt{3}}. \quad (19)$$

Equations (18) (for $V > 0$) and (19) determine $h_1(-\ell_0 \le x \le 0)$ in parametric form. $h_1(0 < x \le \ell_0)$ follows from the symmetry $h(-x, t) = h(x, t)$. The interface develops a cusp singularity at $x = 0$: $h(|x| \ll 1, 1) \simeq H_1 - 2|x|^{1/2}$, where $H_1 = (1/2)(3\pi/2)^{2/3}$. Now we plug this H_1, and s from Eq. (16), into Eq. (11). As a result, Eq. (6) becomes

$$-\ln \mathcal{P} \simeq \frac{8\sqrt{2|\lambda|}}{15\pi D}\frac{H^{5/2}}{T^{1/2}}. \quad (20)$$

The "5/2 tail" is controlled by the nonlinearity and independent of ν. Figure 1 shows that the asymptotic (20) slowly converges to the numerical result at large positive H. Figure 2 shows the optimal time histories of the height profile $h(x, t)$ and of the auxiliary field $\rho(x, t)$, as observed in the full numerical solution for $\Lambda = 10^3$. The analytical predictions agree very well with the numerics except in narrow boundary layers, where diffusion is important. These boundary layers do not contribute to the action in the leading order in H.

(iv) $H \to -\infty$, *or* $\Lambda \to -\infty$.— Here $\rho = \rho_0(x)$ is localized in a small boundary layer (BL) around $x = 0$, and does not depend on time, except very close to $t = 0$ and $t = 1$; see Fig. 3(b). $h(x, t)$ behaves in the BL as $h_0(x, t) = h_0(x) - ct$, where $c = \mathrm{const}$; see Fig. 3(a). Outside the BL $\rho(x, t) \simeq 0$, and $h(x, t)$ obeys the deterministic equation

$$\partial_t h = \partial_x^2 h - (1/2)(\partial_x h)^2. \quad (21)$$

In the BL we should solve two coupled equations: $-c = V_0' - (1/2)V_0^2 + \rho_0$, and $\rho_0' + \rho_0 V_0 = C_1$, where $V_0(x) \equiv h_0'(x)$ and $C_1 = \mathrm{const}$. As $\rho_0(|x| \to \infty) = 0$, we set $C_1 = 0$. The resulting equations are Hamiltonian, $V_0' = \partial_{\rho_0}\mathfrak{H}$ and $\rho_0' = -\partial_{V_0}\mathfrak{H}$, with the Hamiltonian $\mathfrak{H}(V_0, \rho_0) = (\rho_0/2)(V_0^2 - \rho_0 - 2c)$. As $\rho_0(|x| \to \infty) = 0$, we only need the "zero-energy" trajectory, $\rho_0 = V_0^2 - 2c$. Plugging it into the equation for V_0' and solving the simple resulting equation, we obtain $V_0(x) = \sqrt{2c}\tanh(\sqrt{c/2}x)$ and arrive at the BL solution

$$h(x,t) = h_0(x) - ct = 2\ln\cosh(\sqrt{c/2}x) - ct, \quad (22)$$

$$\rho_0(x) = -2c\,\mathrm{sech}^2(\sqrt{c/2}x). \quad (23)$$

The condition $h(0, 1) = -|H|$ yields $c = |H| \gg 1$. Now we calculate the action (7):

$$S \simeq \frac{1}{2}\int_0^1 dt \int_{-\infty}^{\infty} dx\rho_0^2(x) = \frac{8\sqrt{2}}{3}|H|^{3/2}, \quad (24)$$

and, using Eq. (6), obtain the desired $H \to -\infty$ tail:

$$-\ln \mathcal{P} \simeq \frac{8\sqrt{2}\nu|H|^{3/2}}{3D|\lambda|^{1/2}T^{1/2}}. \quad (25)$$

This tail perfectly agrees with the right tail of the GOE TW distribution [9]. For the initially flat KPZ interface this asymptotic was obtained in the long-time limit [9]. We argue that it holds at any time $T > 0$, provided that the right-hand side of Eq. (25) is much larger than unity. The asymptotic (25) rapidly converges to the numerical result, see the right inset of Fig. 1.

Although the BL solution suffices for evaluating $\ln \mathcal{P}$, it does not hold for most of the optimal path $h(x, t)$. This is because $h_0(x)$ in Eq. (22) diverges at $|x| \to \infty$, instead of vanishing there as it should. The remedy comes from two outgoing-traveling-front solutions of Eq. (21) that hold outside of the BL. For $x > 0$ the traveling front (TF) is of the form $h(z) = -2\ln(1 + C_2 e^{-vz})$, where $z = x - vt$, and $v > 0$ and $C_2 > 0$ are constants to be found. Importantly, the TF solution can be matched with the BL solution (22) in their joint region of validity. Indeed, at $|vz| \gg 1$ and $z < 0$, the TF solution becomes

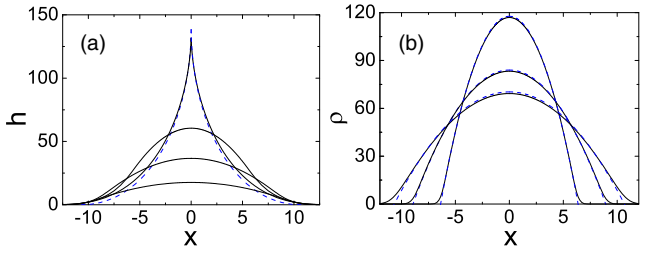

FIG. 2. The optimal interface history for $\Lambda = 10^3$. (a) h vs x for rescaled times $t = 0.25$, 0.5, 0.75, and 1. (b) ρ vs x for $t = 0$, 0.5, and 0.75. Solid lines, numerical; dashed lines, analytical.

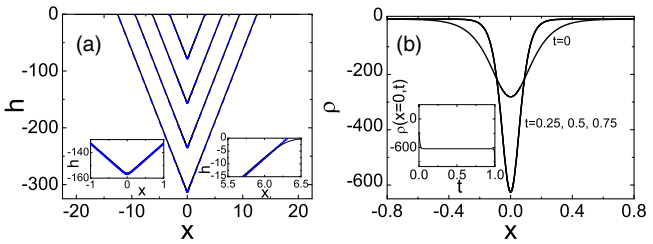

FIG. 3. The optimal interface history for $\Lambda = -10^2$. (a) h vs x for rescaled times t=0.25, 0.5, 0.75, and 1. Insets: the boundary layers at x=0 and at x=$(|H|/2)^{1/2}t$ for t=0.5. (b) ρ vs x for t=0, 0.25, 0.5, and 0.75. Inset: $\rho(x = 0, t)$. The analytical and numerical curves are indistinguishable, except in the insets of (a) and at $t = 0$ for (b).

$$h(x,t) \simeq 2v(x-vt) - 2\ln C_2. \tag{26}$$

In its turn, the outer asymptotic of the BL solution (22), valid at $\sqrt{c}x \gg 1$, is

$$h(x,t) \simeq \sqrt{2c}x - ct - 2\ln 2. \tag{27}$$

Matching Eqs. (26) and (27), we obtain $c = 2v^2$ and $C_2 = 2$. Then, by virtue of the symmetry $h(-x,t) = h(x,t)$, the complete two-front solution is

$$h(x,t) = -2\ln\left[1 + 2e^{-v(|x|-vt)}\right], \quad v = \sqrt{\frac{|H|}{2}} \gg 1. \tag{28}$$

It rapidly decays at $|x| > vt$. Equations (22) and (28) describe the optimal interface history. Notably, the diffusion only acts in the BL (which gives the main contribution to $\mathcal{P}$) and in the small regions of rapid exponential decay. The simple TF solution (27) and its mirror reflection at $x < 0$, which hold in most of the system, are inviscid. Figure 3 shows the optimal time histories of h and ρ obtained numerically and analytically for $\Lambda = -10^2$.

(v) *Low cumulants.*— At short times, $\epsilon \ll 1$, and for sufficiently small rescaled heights H, we can develop a regular perturbation theory in H, or in Λ, cf. [23]. In the zeroth order we have $h_0(x,t) = \rho_0(x,t) = 0$. Therefore,

$$h(x,t) = \Lambda h_1(x,t) + \Lambda^2 h_2(x,t) + \ldots, \tag{29}$$

$$\rho(x,t) = \Lambda\rho_1(x,t) + \Lambda^2\rho_2(x,t) + \ldots. \tag{30}$$

Correspondingly, $S(\Lambda) = \Lambda^2 S_1 + \Lambda^3 S_2 + \ldots$. In the first order, Eqs. (3) and (4) yield

$$\partial_t h_1 = \partial_x^2 h_1 + \rho_1, \tag{31a}$$

$$\partial_t \rho_1 = -\partial_x^2 \rho_1. \tag{31b}$$

Solving the antidiffusion equation (31b) with the boundary condition $\rho_1(x,1) = \delta(x)$, we obtain

$$\rho_1(x,t) = \frac{1}{\sqrt{4\pi(1-t)}} e^{-x^2/4(1-t)}. \tag{32}$$

Therefore, $S_1 = (1/2)\int_0^1 dt \int_{-\infty}^{\infty} dx \rho_1^2(x,t) = (2\sqrt{2\pi})^{-1}$. Now we need to solve the diffusion equation (31a) with the forcing term ρ_1 from Eq. (32) and the initial condition $h_1(x, t=0) = 0$. After standard algebra, the solution is

$$h_1(x,t) = \frac{\sqrt{1+t}e^{-x^2/4(1+t)}}{\sqrt{4\pi}} - \frac{\sqrt{1-t}e^{-x^2/4(1-t)}}{\sqrt{4\pi}} + \frac{x}{4}\operatorname{erf}\left(\frac{x}{2\sqrt{1+t}}\right) - \frac{x}{4}\operatorname{erf}\left(\frac{x}{2\sqrt{1-t}}\right). \tag{33}$$

At $t = 1$ the interface develops a corner singularity at the maximum point $x = 0$:

$$h_1(x, t=1) = \frac{e^{-x^2/8}}{\sqrt{2\pi}} + \frac{x}{4}\operatorname{erf}\left(\frac{x}{2\sqrt{2}}\right) - \frac{|x|}{4}, \tag{34}$$

and we obtain $\Lambda = \sqrt{2\pi}H$, and $S \simeq \Lambda^2/(2\sqrt{2\pi}) = (\pi/2)^{1/2}H^2$. That is, at short times, small height fluctuations are Gaussian [10]. The KPZ nonlinearity kicks in in the second order of the perturbation theory, but the equations for h_2 and ρ_2 are linear:

$$\partial_t h_2 = \partial_x^2 h_2 - (1/2)(\partial_x h_1)^2 + \rho_2, \tag{35}$$

$$\partial_t \rho_2 = -\partial_x^2 \rho_2 - \partial_x(\rho_1 \partial_x h_1), \tag{36}$$

with the boundary conditions $h_2(x,0) = \rho_2(x,1) = 0$. Straightforward but tedious calculations [19] lead to

$$S \simeq \sqrt{\pi/2}H^2 + \sqrt{\pi/72}(\pi - 3)H^3. \tag{37}$$

Then Eq. (6) yields (still in the rescaled variables)

$$\mathcal{P}(H) \sim e^{-(\sqrt{\pi}/\epsilon\sqrt{2})H^2 - (\sqrt{\pi}/\epsilon\sqrt{2})[(\pi-3)/6]H^3 + (1/\epsilon)\mathcal{O}(H^4)} = e^{-(\sqrt{\pi}/\epsilon\sqrt{2})H^2}\left[1 - \frac{\sqrt{\pi}}{\epsilon\sqrt{2}}\frac{\pi-3}{6}H^3 + \frac{\mathcal{O}(H^4)}{\epsilon}\right]. \tag{38}$$

This distribution holds when $\nu^{1/2}H^2/(D\sqrt{T}) \gg 1$ and $|\lambda|H/\nu \lesssim 1$. The second and third cumulants of $\mathcal{P}$, in the leading order in ϵ, are

$$\kappa_2 \simeq D\sqrt{\frac{T}{2\pi\nu}}, \qquad \kappa_3 \simeq \frac{(\pi-3)D^2\lambda T}{4\pi\nu^2}, \tag{39}$$

in agreement with Ref. [10]. The left inset of Fig. 1 compares, for moderate H, Eq. (37) with our numerical results [24].

(vi) *Discussion.*—Let us summarize the predictions of the WNT. At short times, $\epsilon \ll 1$, the dependence of $S \simeq -\epsilon \ln \mathcal{P}(H,T)$ on H (in the proper moving frame [17]) is shown in Fig. 1. The body of the distribution is described by Eq. (38) (see also Ref. [9]); the tails are described by Eqs. (20) and (25). The small parameter $\epsilon \ll 1$ guarantees the validity of these results at all H.

At long but fixed time, $\epsilon \gg 1$, the WNT is not valid in the body of the height distribution, giving way to the GOE TW statistics [9]. Far in the tails, however, the action S is very large. Therefore, we argue that the WNT tails (20) and (25) hold. The $3/2$ tail is captured by the TW statistics, the $5/2$ tail is not. We expect the $5/2$ tail to hold when it predicts a much higher probability than the left tail, $-\ln\mathcal{P} \sim \nu^2 H^3/(|\lambda|D^2 T)$, of the TW distribution. The condition is $H \gg D^2|\lambda|^3 T/\nu^4$.

Hopefully, the $5/2$ tail will be observed in experiments and extracted from the exact solution [9]. Notably, a 2.4 ± 0.2 tail (and a 1.6 ± 0.2 tail) were observed in numerical simulations of directed polymers in a random potential [25]. Also, the $5/2$ and $3/2$ tails were obtained for the

current statistics of the TASEP in a ring [26]. To what extent the latter, finite-system results are related to our infinite-system results is presently under study.

We thank P. Le Doussal, T. Halpin-Healy, P. L. Krapivsky, S. Majumdar, and P. V. Sasorov for useful discussions. B. M. acknowledges financial support from the United States-Israel Binational Science Foundation (BSF) (Grant No. 2012145).

Note added in proof.—Recently, we learned that distribution tails equivalent to our Eqs. (20) and (25) were obtained in Ref. [27] in the context of directed polymer statistics.

*meerson@mail.huji.ac.il
†eytan.katzav@mail.huji.ac.il
‡vilenkin@mail.huji.ac.il

[1] M. Kardar, G. Parisi, and Y.-C. Zhang, Phys. Rev. Lett. **56**, 889 (1986).
[2] T. Halpin-Healy and Y.-C. Zhang, Phys. Rep. **254**, 215 (1995); T. Halpin-Healy and K. A. Takeuchi, J. Stat. Phys. **160**, 794 (2015).
[3] A.-L. Barabasi and H. E. Stanley, *Fractal Concepts in Surface Growth* (Cambridge University Press, Cambridge, England, 1995).
[4] J. Krug, Adv. Phys. **46**, 139 (1997).
[5] J. Quastel and H. Spohn, J. Stat. Phys. **160**, 965 (2015).
[6] H. Spohn, arXiv:1601.00499.
[7] Changing λ to $-\lambda$ is equivalent to changing h to $-h$.
[8] W. M. Tong and R. W. Williams, Annu. Rev. Phys. Chem. **45**, 401 (1994); L. Miettinen, M. Myllys, J. Merikoski, and J. Timonen, Eur. Phys. J. B **46**, 55 (2005); M. Degawa, T. J. Stasevich, W. G. Cullen, A. Pimpinelli, T. L. Einstein, and E. D. Williams, Phys. Rev. Lett. **97**, 080601 (2006); K. A. Takeuchi and M. Sano, Phys. Rev. Lett. **104**, 230601 (2010); J. Stat. Phys. **147**, 853 (2012); K. Takeuchi, M. Sano, T. Sasamoto, and H. Spohn, Sci. Rep. **1**, 34 (2011).
[9] P. Calabrese and P. Le Doussal, Phys. Rev. Lett. **106**, 250603 (2011); P. Le Doussal and P. Calabrese, J. Stat. Mech. (2012) P06001.
[10] T. Gueudré, P. Le Doussal, A. Rosso, A. Henry, and P. Calabrese, Phys. Rev. E **86**, 041151 (2012).
[11] P. C. Martin, E. D. Siggia, and H. A. Rose, Phys. Rev. A **8**, 423 (1973).
[12] M. I. Freidlin and A. D. Wentzell, *Random Perturbations of Dynamical Systems* (Springer-Verlag, New York, 1998).
[13] G. Falkovich, K. Gawędzki, and M. Vergassola, Rev. Mod. Phys. **73**, 913 (2001); T. Grafke, R. Grauer, and T. Schäfer, J. Phys. A **48**, 333001 (2015).
[14] L. Bertini, A. De Sole, D. Gabrielli, G. Jona-Lasinio, and C. Landim, Rev. Mod. Phys. **87**, 593 (2015).
[15] V. Elgart and A. Kamenev, Phys. Rev. E **70**, 041106 (2004); B. Meerson and P. V. Sasorov, Phys. Rev. E **83**, 011129 (2011); **84**, 030101(R) (2011).
[16] H. C. Fogedby, Phys. Rev. E **59**, 5065 (1999); H. C. Fogedby and W. Ren, Phys. Rev. E **80**, 041116 (2009).
[17] The solution of Eq. (1) includes a systematic interface displacement $h_s(t)$ that comes from the rectification of the noise by the nonlinearity [6,10,18]. At long times $\dot{h}_s(t)$ approaches a constant that depends on the small-scale cutoff. Our $H(t)$ is defined as $H(t) = h(0,t) - h_s(t)$.
[18] M. Hairer, Ann. Math. **178**, 559 (2013).
[19] See Supplemental Material at http://link.aps.org/supplemental/10.1103/PhysRevLett.116.070601 for a brief derivation of the weak-noise equations and calculation of higher-order terms of the expansion of $S(H)$ at small H.
[20] A. I. Chernykh and M. G. Stepanov, Phys. Rev. E **64**, 026306 (2001).
[21] B. Meerson and P. V. Sasorov, Phys. Rev. E **89**, 010101(R) (2014).
[22] L. D. Landau and E. M. Lifshitz, *Fluid Mechanics* (Reed, Oxford, 2000).
[23] P. L. Krapivsky and B. Meerson, Phys. Rev. E **86**, 031106 (2012).
[24] The first cumulant of $\mathcal{P}(H,T)$ from Eq. (38) has the same parameter dependence, as the one derived in Ref. [10], but a different numerical coefficient. This suggests that the WNT misses a short-wavelength contribution to the systematic interface displacement.
[25] J. M. Kim, M. A. Moore, and A. J. Bray, Phys. Rev. A **44**, 2345 (1991).
[26] B. Derrida and J. L. Lebowitz, Phys. Rev. Lett. **80**, 209 (1998); B. Derrida and C. Appert, J. Stat. Phys. **94**, 1 (1999).
[27] I. V. Kolokolov and S. E. Korshunov, Phys. Rev. B **75**, 140201(R) (2007); **78**, 024206 (2008); **80**, 031107 (2009).